REPORT DOCUMENTATION PAGE		Form Approved OMB No. 0704-0188

Public reporting burden for this collection of information is estimated to average 1 hour per response, including the time for reviewing instructions, searching existing data sources, gathering and maintaining the data needed, and completing and reviewing the collection of information. Send comments regarding this burden estimate or any other aspect of this collection of information, including suggestions for reducing the burden, to Department of Defense, Washington Headquarters Services, Directorate for Information Operations and Reports (0704-0188), 1215 Jefferson Davis Highway, Suite 1204, Arlington, VA 22202-4302. Respondents should be aware that notwithstanding any other provision of law, no person shall be subject to any penalty for failing to comply with a collection of information if it does not display a currently valid OMB control number.
PLEASE DO NOT RETURN YOUR FORM TO THE ABOVE ADDRESS.

1. REPORT DATE (DD-MM-YYYY) 31-03-2004	2. REPORT TYPE Final Report	3. DATES COVERED (From – To) 16-09-2002 – 31–03-2004

4. TITLE AND SUBTITLE	5a. CONTRACT NUMBER
Amorphous, Porous and Black Silicon for Photonic Applications	FA8655-02-M4086
	5b. GRANT NUMBER
	5c. PROGRAM ELEMENT NUMBER

6. AUTHOR(S)	5d. PROJECT NUMBER
Dr. Ali Serpenguzel	
	5d. TASK NUMBER
	5e. WORK UNIT NUMBER

7. PERFORMING ORGANIZATION NAME(S) AND ADDRESS(ES) Koc University Rumeli Feneri Yolu, Science Building, Room 161 Sariyer 80910 Turkey	8. PERFORMING ORGANIZATION REPORT NUMBER N/A

9. SPONSORING/MONITORING AGENCY NAME(S) AND ADDRESS(ES) EOARD PSC 802 BOX 14 FPO 09499-0014	10. SPONSOR/MONITOR'S ACRONYM(S)
	11. SPONSOR/MONITOR'S REPORT NUMBER(S) SPC 02-4086

12. DISTRIBUTION/AVAILABILITY STATEMENT

Approved for public release; distribution is unlimited.

13. SUPPLEMENTARY NOTES

14. ABSTRACT

This report results from a contract tasking Koc University as follows: The contractor will investigate photoluminescence and optical reflection, transmission and absorption in three types of silicon -- amorphous, porous, and "black" silicon, and correlate the optical properties with morphological features. All three types of silicon exhibit strong luminescence and novel optical properties. These forms of silicon could potentially lead to new optical, photonic and electrical devices such as heads-up displays, optical detectors, and optical switches for telecommunications.

15. SUBJECT TERMS
EOARD, Photonics, silicon, photoluminescence

20040715 176

16. SECURITY CLASSIFICATION OF:			17. LIMITATION OF ABSTRACT UL	18, NUMBER OF PAGES 38	19a. NAME OF RESPONSIBLE PERSON CHARLES H. WARD, Lt Col, USAF
a. REPORT UNCLAS	b. ABSTRACT UNCLAS	c. THIS PAGE UNCLAS			19b. TELEPHONE NUMBER (Include area code) +44 (0)20 7514 3154

Standard Form 298 (Rev. 8/98)
Prescribed by ANSI Std. Z39-18

DEPARTMENT OF THE AIR FORCE

EUROPEAN OFFICE OF AEROSPACE RESEARCH AND DEVELOPMENT
(EOARD)

AMORPHOUS, POROUS, AND BLACK SILICON
FOR PHOTONIC APPLICATIONS

EOARD Special Contract SPC-024086
Contract Order Number FA8655-02-M-4086

Final Report

DTIC Copy

Dr. Ali Serpengüzel, Principal Investigator
Koc University, Microphotonics Research Laboratory
Department of Physics, Rumeli Feneri Yolu
Science Building, Sariyer 34450 Istanbul - Turkey

Voice: +90 (212) 338-1312
Facsimile: +90 (212) 338-1547
E-mail: aserpenguzel@ku.edu.tr
URL: http://microphotonics.ku.edu.tr

AQ F04-09-1613

Physics & Astronomy Classification Scheme (PACS)* codes:

(71.23.Cq) Amorphous semiconductors, metallic glasses, glasses;
(73.61.Jc) Amorphous semiconductors; glasses;
(78.66.Jg) Amorphous semiconductors; glasses; nanocrystalline materials;
(78.55.-m) Photoluminescence.

*http://www.aip.org

Optics Classification & Indexing Scheme (OCIS)** codes:

(230.0250) Optoelectronics;
(250.5230) Photoluminescence;
(300.2530) Laser induced fluorescence,
(310.0310) Thin films;

**http://www.osa.org

Keywords:

Amorphous silicon,
Black silicon,
Luminescence,
Non-crystalline silicon,
Porous silicon,
Optoelectronics,
Photoluminescence,
Silicon,
Spontaneous emission,
Thin films.

Preface

The report comprises the results obtained from the 'Amorphous, porous, and black silicon for photonic applications' EOARD Special Contract SPC-024086, Contract Order Number FA8655-02-M-4086. The purpose of this project is the spectroscopic characterization of the amorphous, porous, and black silicon for optoelectronic applications. These silicon based materials are morphologically similar to each other, and have similar luminescence properties.

Amorphous silicon is grown by plasma enhanced chemical vapor deposition (PECVD) on silicon substrates. Porous silicon is obtained from crystalline silicon by electrochemical etching. Black silicon is obtained from crystalline silicon by femtosecond laser processing. The temperature dependence of the amorphous, porous, and black silicon photoluminescence is performed to fully characterize and optimize the material in the pursuit of obtaining novel photonic microdevices. Atomic force microscopy (AFM) is used for morphological material characterization. Such fundamental studies are important for the development of novel optoelectronic devices with increased efficiency, speed, and bandwidth.

Photonic devices manufactured using amorphous, porous, and black silicon have potential optoelectronic applications such as flat panel or heads-up displays, wavelength division multiplexing (WDM) light sources and detectors, nanocavity lasers, optical add-drop filters, optical couplers and waveguides, and diffractive optical elements. Currently, these devices exist as discrete photonic elements. However, in the near future, they will be integrated into nanofabricated photonic integrated circuits (PIC's) operating at visible and near-infrared (near-IR) wavelengths. These integrated devices are essential for the high speed and high capacity information superhighway. With the incorporation of integrated services digital network (ISDN) architecture into our daily environment, we will need this optical communication infrastructure in the next decade. Additional device applications may include physical, chemical, and biological agent detection.

Properties of amorphous, porous, and black silicon, as well as characterization techniques are introduced in Chapter 1. Amorphous silicon is studied in detail in Chapter 2. Porous silicon is studied in detail in Chapter 3. Black silicon is studied in detail in Chapter 4. Finally, Chapter 5 concludes the work. As the principal investigator of this project, I would like to acknowledge the support of our Laboratory engineer, Adnan Kurt, and my graduate students Temel Bilici, Senol Isci, Ibrahim Inanç, and Yigit Ozan Yilmaz.

Istanbul, March, 2004   *Ali Serpengüzel*

Contents

List of Figures

List of Tables

1. Introduction

Crystalline silicon being ubiquitous throughout the microelectronics industry has an indirect bandgap, and therefore is incapable of light emission. However, strong room temperature visible and near-IR luminescence from non-crystalline silicon, e.g., amorphous silicon, porous silicon, and black silicon, has been observed. These silicon based materials are morphologically similar to each other, and have similar luminescence properties. We have studied the temperature dependence of the photoluminescence from these non-crystalline silicons to fully characterize and optimize these materials in the pursuit of obtaining novel optoelectronic devices.

Interest in silicon (Si) as a material for optoelectronics has increased recently. With modern process techniques, it will be possible to integrate lasers, photodetectors, and waveguides into optoelectronic silicon motherboards to route and modulate optical signals within such silicon motherboards. Integrated silicon optoelectronics is a rapidly developing field [1]. Discrete and integrated devices such as photodetectors, modulators, light emitters, resonant cavity enhanced (RCE) photodetectors, waveguides, photonic bandgap filters, optical amplifiers, optical interconnects, and optoelectronic integrated circuits are already being realized. However, most of these devices, with the exception of light emitters, are fabricated using crystalline silicon. Light emission requires the use of amorphous silicon, since crystalline silicon can not emit light due to its indirect bandgap.

1.1. Amorphous silicon

In the optoelectronics and microelectronics industry silicon is the most widely used semiconductor, not only in its crystalline, but also in its amorphous form. Being a direct band-gap material, [2] unlike crystalline silicon, [3] amorphous silicon is unmatched as a photoreceptor for laser printing, for switching elements in large area liquid crystal displays, for large photovoltaic panels, and any other application that calls for a high quality semiconductor that can be processed on large areas or on curved or flexible substrates. It is generally agreed that the terms amorphous solid, non-crystalline solid, disordered solid, glass, or liquid have no precise structural meaning beyond the description that, the structure is not crystalline on any significant scale. The principal structural order present is imposed by the approximately constant separation of nearest-neighbor atoms or molecules.

Until the early 1970's, amorphous silicon prepared by evaporation or sputtering was not considered as one of the valuable semiconductor materials, because of high density of electronic states in the band gap related to a large density of structural defects. [4] The discovery of an amorphous silicon material prepared by the glow discharge deposition of silane, which can be doped and whose conductivity can be changed by ten orders of magnitude marked a turning point and opened a new research area.

Most interest focused on hydrogenated amorphous silicon and its alloys, since hydrogen by removing dangling bonds eliminates non-radiative recombination centers, that are responsible for reduced luminescence efficiency (and reduced photovoltaic efficiency) and allows doping. [5] Another advantage of the hydrogenated amorphous silicon is that, it can be deposited by plasma enhanced chemical vapor deposition (PECVD) onto almost any substrate at temperatures below 500 K, which makes it compatible with the microelectronic technology.

1.2. Porous Silicon

Similar to hydrogenated amorphous silicon, porous silicon also exhibits room temperature visible PL [6]. Semiconductor microcavity effects have been applied to porous silicon, after the observation of room temperature visible PL [7] made porous silicon a potential optical gain medium [8]. Steady state [9, 10, 11] and temporally resolved, [12] single and multiple[13] microcavity controlled PL in porous silicon has been observed experimentally [14, 15, 16] and calculated theoretically [17]. The possibility of using porous silicon microcavities as chemical sensors has been investigated [18]. In addition, microcavity controlled PL has been observed in porous silicon inorganic-organic structures [19], as well as Si/SiO_x superlattices [20, 21, 22]. SiO_2/TiO_2 microcavities [23], SiO_x/WO_y, and SiO_x/MO_y multilayers [24] have been fabricated. Microcavity controlled electroluminescence (EL) of porous silicon has been reported [25, 26]. Interference filters [27] and optical waveguides [28] have also formed from porous silicon. Two-dimensional (2-D) photonic crystals have been fabricated in porous silicon [29] and silicon nitride [30] waveguides.

1.3. Black Silicon

Silicon is the material of computer chips and solar cells. It is ubiquitous throughout the high-tech world. Ordinarily, silicon absorbs a moderate amount of visible light, but a substantial amount of visible light is reflected as well, and infrared and ultraviolet light are transmitted through silicon or reflected from it with very little absorption. Spiked silicon surfaces, in contrast, absorb nearly all light at wavelengths ranging from the ultraviolet to the infrared. This suggests it may be very useful in improving the performance of existing silicon devices, such as detectors and photovoltaics. Spiked silicon is made by shining a series of very short, very intense laser pulses at a silicon surface in a chamber filled with a gas such as sulfur hexafluoride or chlorine. In the presence of the laser light, the gas reacts with the silicon surface etches away some of it, leaving a pattern of conical spikes behind. Mazur's group recently [31,32] discovered that irradiation of silicon surfaces with femtosecond laser pulses in the presence of a halogen containing gas transforms the flat, mirror-like surface of a silicon wafer into a forest of microscopic spikes. The spiked surface is strongly light-absorbing: the surface of silicon, normally gray and shiny, turns deep black. The spikes are tens of micrometers tall and have tip sizes on the order of hundreds of nanometers.

1.4. Sample Cleavage, Cleaning and Cleanliness

In the field of device physics cleaning means to remove the undesired materials from the wafer before each process step. The dirt may come either from the surroundings or from the previous process steps. Cleanliness is to prevent the contamination and to maintain the level of cleanliness

that is already present. These two definitions are in fact very simple, but they are very crucial for achieving high performances in the production of semiconductor devices.

Clean rooms are categorized by the number of particles contained in the air. A clean room categorized as a class-100 clean room has 100 or less particles that are 0.5 micrometer or greater in diameter, in a cubic foot of air. A class-100, which is used for fabrication of semiconductor devices, requires good filtering techniques and protective clothing on personnel. Class-10000, which is relatively easy to obtain, is generally used for semiconductor characterization. For comparison, the general environment of an average building usually exceeds class-100000.

Because we fabricate our devices in just one step, cleaning operation is performed once, after cleaving. The wafers are cleaved into pieces of dimensions 2.0 x 2.0 cm^2 to fit them into our reflectance measurement setup. This size is also big enough to assume in theoretical calculations, that the cavity has infinite dimensions in the x -y plane. In our processes, we performed 3-solvent cleaning, in which the solvents are Tricholoroethan (TCE), Aceton (ACE), and Isopropyl Alcohol (ISO). The samples were boiled for 2 minutes in TCE, and then left at room temperature and then rinsed with deionized water. Drying is very important such that no droplets should be evaporated on the surface, since they carry dirt. For this reason nitrogen gun is used for removing the water from the surface. Finally the samples are kept on the hot plate at 120°C for 50 seconds. The solvents are semiconductor grade, that is they are extremely pure and filtered in sub-microns. Organic solvents are effective in removing oils, greases, waxes and organic materials. Many cleaning methods with various materials procedures do exist, and they are chosen by trial and error.

1.5. Plasma Enhanced Chemical Vapor Deposition

Plasma processing is used extensively in the semiconductor industry for etching and growth of thin film materials [33]. Plasma assisted techniques are especially important in deposition of thin-film materials because they can be accomplished at relatively low temperatures. Such materials could be deposited on wafers using chemical vapor deposition, in which the reactant species are introduced into the vicinity of a hot wafer by gaseous flow and the appropriate reactions to drive this chemical reactions are often 700° to 1000° C. For gallium arsenide wafers, arsenic evolves in this temperature range. Metals commonly present on the wafer can not be exposed to these extremes either. As one example ohmic constants are formed at approximately 450° C. Temperatures above 500° C will rapidly destroy the ohmic contact. Therefore CVD is not a generally useful technique, so low-temperature, plasma driven reactions are used instead. The plasma-assisted deposition process is denoted as plasma-enhanced chemical vapor deposition (PECVD). PECVD yields films that are amorphous in nature with very little short range structural ordering. Chemical bonding within the film may vary. The plasma assisted deposition process sometimes has been called plasma polymerization to emphasize that the film may be randomly bonded, and highly cross-linked. Therefore, chemical species other than the desired ones are often included in the film. In this sense, plasma assisted deposition is more complex than plasma-assisted etching, in which it does not much matter what the final products are, because they disappear into the pumps.

From the perspective of a physicist, the plasma state encompasses a wide range of electron energies and densities and includes such phenomena as flames, low-pressure arcs, solar coronas, and thermonuclear reactions. The regime of interest to semiconductor processing is the low-pressure plasma or glow discharge regime. These plasmas are characterized by gas pressures on the order of 0.1 to several Torr, free-electron densities of 10^9 to 10^{12} cm^{-3}, and electron energies of 1.0 to 10.0 e V.

The plasma is able to generate chemically reactive species at relatively low temperature because of the nature of the plasma state. The temperature of the chemical species (atoms, molecules, or radicals), as represented by their translational and rotational energy, is generally near ambient. The electrons, however, can exhibit temperatures of tens of thousands of degrees Kelvin. The electron energy is sufficient to break molecular bonds and create chemically active species in the plasma. Any of these species can be excited to higher electronic energy states by further interaction with the electrons. Hence, chemical reactions that usually occur only at high temperatures can be made to occur at low or even ambient temperatures in the presence of an activating plasma state. Most of the species remain neutral in glow discharges. This feature allows most of the plasma to remain near ambient temperatures. Although the ionization rate is small, it is adequate to provide sufficient number of reactive species. The light glow emitted from the plasma is characteristic of the electronic transitions taking place. The wafer is generally heated to aid the deposition process, but usually less than a few hundred degrees Celsius.
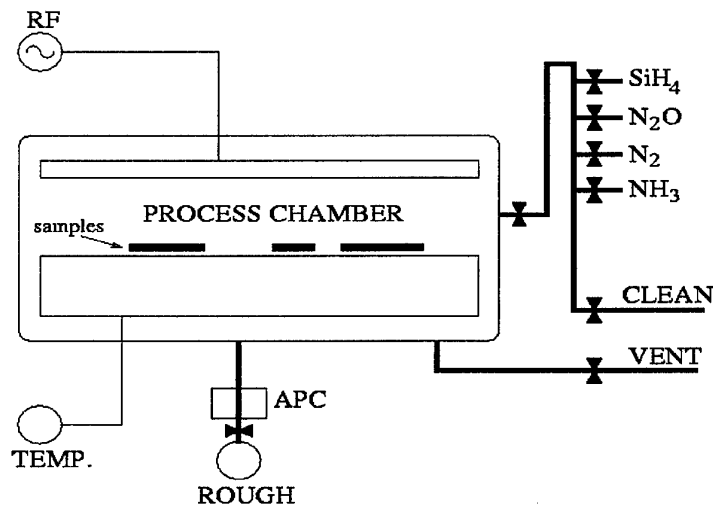

Figure 1.1. The schematic of the Plasma Enhanced Chemical Vapor Deposition (PECVD) system.

Plasma processing occurs in equipment called plasma reactors. Wafers are placed on the lower electrode, which is also used to heat wafers. The 13.56 MHz RF signal which excites the plasma is applied across the two electrodes. The reactant gases are introduced at the outer radius, and flow radially between the electrodes. The plasma occupies the region between the two electrodes, but is excluded from the immediate vicinity of the electrode surface by electromagnetic effects. This region is called the plasma sheath or the dark region (because it doesn't glow). It is on the order of 0.1 to 10.0 mm thick, depending on the operating conditions. The plasma is generally neutral, with positive species balancing negative ones. However, the plasma sheath is a region of positive space charge and the electrode surfaces are negative with

respect to the plasma. This is due to the higher mobility of electrons, which move rapidly to the surface of electrodes. The RF voltage is applied through a large blocking capacitor, so that no dc bias is intentionally applied. Most of the voltage between the two electrodes is dropped across the two plasma sheaths.

The plethora of chemical species in the plasma and the nature of the plasma state make processing results extremely sensitive to virtually all possible parameters: gas type, gas flow rate, gas delivery position, pressure, electrode geometry, power, power density, radio frequency, wafer temperature, and wafer material The possible chemical reactions can be highly complex, because of the presence of so many radicals. These considerations mean that plasma processes are developed more by empirical means than by theoretical analysis.

1.6. Photoluminescence measurements

Photoluminescence (PL) study of a sample is a good technique to characterize the material, revealing the optical characteristics of the sample. To investigate the light emission properties of the sample, a PL spectrum is necessary. This analysis helps in understanding the energy band structure of the sample, therefore determining the emission wavelength, together with some other material parameters. The interaction of light with semiconductors occur at the spectral range 0.1-1000 μm (0.001-12 eV). In the near ultraviolet, visible, near infrared region (0.24-3.1 eV) the dominant effect is absorption at the band gap and by impurities, leading to PL under certain conditions.
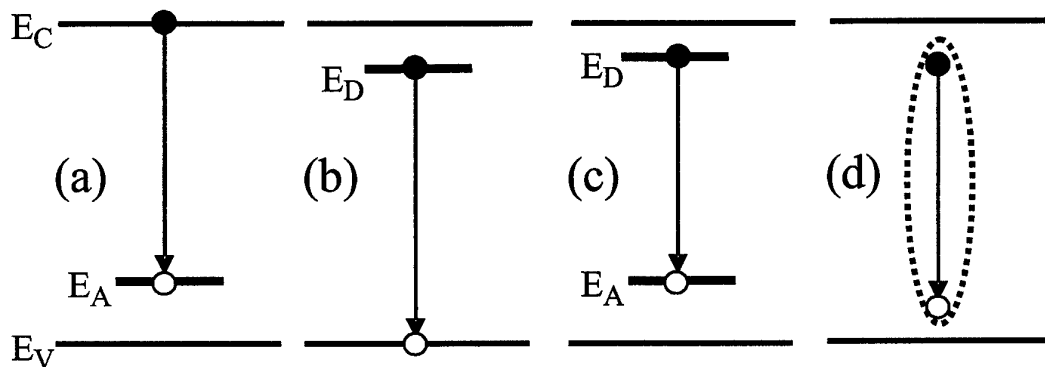

Figure 1.2. Radiative recombination processes involving impurity levels. (a) conduction-band acceptor transition, (b) Donor valence-band transition, (c) donor acceptor recombination, (d) free-exciton recombination.

A valence electron can be excited across the band gap of a semiconductor with an incoming photon, whose energy equals to or exceeds the gap value. Absorption also occurs, when the photon raises an electron from a neutral donor level to the conduction band, or from the valence band to a neutral acceptor level. It is also possible to induce absorptive transition from the valence band to an ionized donor level, or from an ionized acceptor level to the conduction band. These processes lead to the sensitive probe of PL, which occurs when the excited electron returns to its initial state. This process can be either radiative or non-radiative. If it is radiative, it emits a

photon whose energy gives the difference between the excited and the initial state energies. The emission spectrum shows a fingerprint peak related to the energy of each excited level.
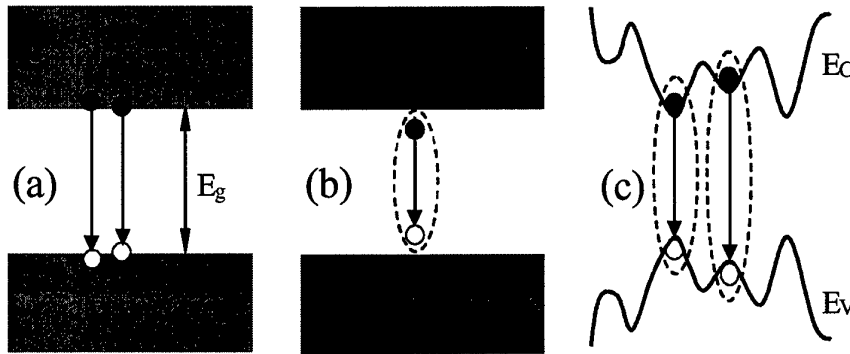

Figure 1.3. Radiative transitions in semiconductors. (a) band-to-band transitions; (b) free-exciton annihilation; (c) recombination of exciton localized at band-potential fluctuations.

The gap being direct or indirect strongly affects the absorption process. The incoming photon carries negligible momentum compared to that of the electron, so the absorbing electron gains energy without changing its wavevector. In a direct gap semiconductor like GaAs an electron at the valence band maximum, executes a vertical transition to the conduction band minimum directly above. From the energy conservation, $h\nu = Ef - Ei$, where Ef and Ei are the final and initial energies of the electron, and $h\nu$ is the photon energy.
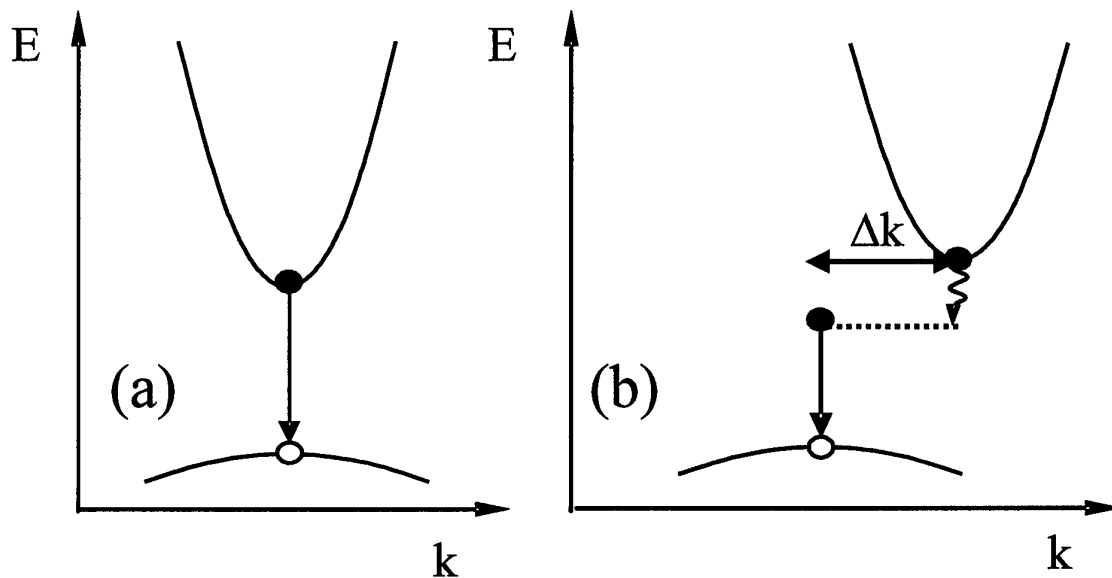

Figure 1.4. (a) Vertical band-to-band radiative transition in direct gap semiconductor; (b) phonon assisted radiative transition in indirect gap semiconductor.

For an indirect gap semiconductor like crystalline silicon, the excited electron needs additional momentum to reach the conduction band minimum at a nonzero wavevector. It gains this momentum through a phonon, $h\nu = E_f - E_i \pm hk$, where hk is the phonon energy, and $\pm$ corresponds to the phonon emission and absorption. Phonon emission dominates at low temperatures, since there are less phonons. The need for an additional third body interaction with the phonon makes indirect absorption far less probable then direct absorption, resulting in a weak absorption.

After any of the absorption processes separates an electron and a hole, they recombine. This can proceed in either radiative or non-radiative form. In a direct gap semiconductor, the recombination transition is vertical. For an indirect gap, a phonon must be involved as in indirect absorption. Because of the same reason, as in absorption, the indirect recombination process is much less probable than direct recombination. This explains why crystalline silicon, with its indirect band gap, is a poor light emitter.

Although radiative emission is in many ways the inverse of absorption, there are two main distinctions. One is that recombination is a non-equilibrium process, requiring a supply of electrons at energies above their equilibrium values. For this reason lasers are used as pumping sources. Second, all electronic states whose energy difference obey the conservation law participate in absorption, leading to broad spectral features. But for emission, the recombining electron hole pairs have well defined energy levels, resulting in narrow spectral features. This is why PL is a better tool for characterization than absorption spectroscopy. The sharp peaks of PL can yield highly accurate values for the gap and impurity energies.

The room temperature PL setup consists of a pump laser, a spectrometer, a lock-in amplifier, and a digital oscilloscope. The collected PL signal is imaged to the entrance slit of the spectrometer, whose output is fed to a sensitive photomultiplier tube (PMT). A lock-in-amplifier is providing the necessary electronic gain to the PMT output gain in phase with the laser pulse. The digital oscilloscope is used for monitoring and optimizing the PMT signal. All of the measurement and test devices are computer controlled and the data is acquired digitally. For the room temperature measurements at 300 K the samples are attached to a holder. For low temperature measurements the samples are placed in a closed cycle cryostat system. The closed cycle cryostat system is used to control the sample temperature from 10 K to 300 K.
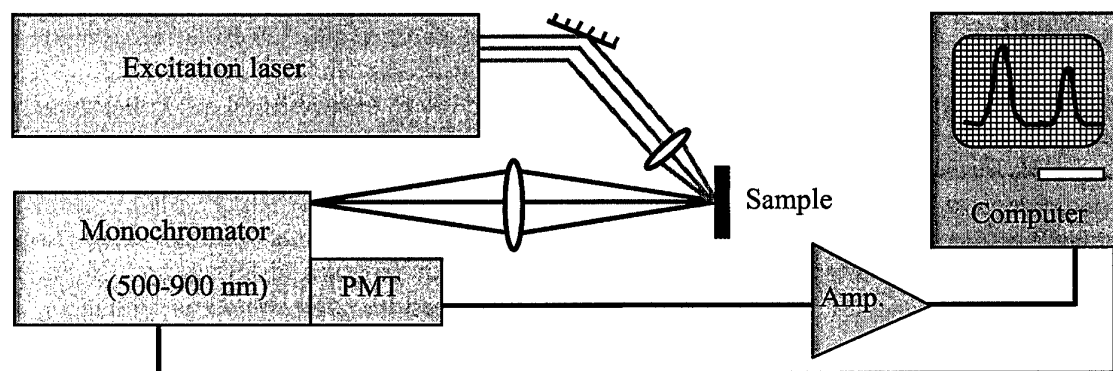

Figure 1.5. The experimental photoluminescence setup.

1.7. References

[1]   H. Zimmermann, "Integrated Silicon Optoelectronics," (Springer Verlag, Berlin, 2000) pp. 1-352.

[2]   J.D. Joannopoulos and G. Lucovsky, "The physics of hydrogenated amorphous silicon," (Springer Verlag, Berlin, 1984).

[3]   S. Perkowitz, "Optical Characterization of Semiconductors," (Academic Press, London, 1993), p.27.

[4]   P. Shaoqi and D. Xiaoning, "Properties of Sputtered Amorphous Silicon without Hydrogen", in *"Proceedings of the International Workshop on Amorphous Semiconductors,"* H. Fritzsche, D. Han, C. C. Tsai, Eds. (World Scientific, Singapore, 1987).

[5]   J. I. Panvoke, "Luminescence in Hydrogenated Amorphous Silicon", in *"Proceedings of the International Workshop on Amorphous Semiconductors,"* H. Fritzsche, D. Han, C. C. Tsai, Eds., (World Scientific, Singapore, 1987).

[6]   D. J. Wolford, B. A. Scoot, J. A. Reimer and J. A. Bradley, "Efficient visible luminescence from hydrogenated amorphous silicon," Physica **B 117**, 920 (1983).

[7]   T. Canham, "Silicon Quantum Wire Array Fabrication by Electrochemical and Chemical Dissolution of Wafers," Appl. Phys. Lett. **57**, 1046 (1990).

[8]   D. J. Lockwood, "Optical Properties of Porous Silicon," Solid State Commun. **92**, 101 (1994).

[9]   L. Pavesi, C. Mazolleni, A. Tredicucci, and V. Pellegrini, "Controlled photon emission in porous silicon microcavities," Appl. Phys. Lett. **67**, 3280 (1995).

[10]   L. Pavesi and V. Mulloni, "All porous silicon microcavities: growth and physics," J. Lumin. **80**, 43 (1999).

[11]   M. Araki, H. Koyama, and N. Koshida, "Precisely tuned emission from porous silicon vertical optical cavity in the visible region," J. Appl. Phys. **80**, 4841 (1996).

[12]   M. Cazzanelli and L. Pavesi, "Time-resolved photoluminescence of all porous silicon microcavities," Phys. Rev. B **56**, 15264 (1997).

[13]   E. K. Squire, P. A. Snow, P. St. J. Russell, L. T. Canham, A. J. Simmons, and C. L. Reeves, "Light emission from porous silicon single and multiple cavities," J. Lumin. **80**, 125 (1999).

[14]   M. Takahashi, Y. Toriumi, T. Matsumoto, Y. Masumoto, N. Koshida, "Significant photorefractive index change observed in porous silicon Fabry-Perot resonators," Appl. Phys. Lett. **76**, 1990 (2000).

[15]   S. Setzu, S. Letant, P. Solsona, R. Romestain, and J. C. Vial, " Improvement of luminescence in p-type as-prepared or dye impregnated porous silicon microcavities," J. Lumin. **80**, 129 (1999).

[16]   Z. H. Xiong, S. Yuan, Z. M. Jiang, J. Qin, C. W. Pei L. S. Liao, X. M. Ding, X. Y. Hou, and X. Wang, "Photoluminescence studies of porous silicon microcavities," J. Lumin. **80**, 137 (1999).

[17]   E. K. Squire, P. St. J. Russell, and P. A. Snow, "Optimized light emission from layered porous silicon structures," Appl. Opt. **37**, 7107 (1998).

[18]   V. Mulloni and L. Pavesi, "Porous silicon microcavities as optical chemical sensors," Appl. Phys. Lett. **76**, 2523 (1999).

[19]   A. Arena, S. Patane, G. Saitta, S. Savasta, R. Girlanda, and R. Rinaldi, "Silicon based organic-inorganic microcavity and its dispersion curve from angle resolved photoluminescence," Appl. Phys. Lett. **72**, 2571 (1998).

[20]   B. T. Sullivan, D. J. Lockwood, H. J. Labbe, and Z.-H. Lu, "Photoluminescence in Amorphous Si/SiOx Superlattices Fabricated by Magnetron Sputtering," Appl. Phys. Lett. **69**, 3149 (1996).

[21]   D. J. Lockwood, J.M. Baribeau, and B. T. Sullivan, "Visible light from Si/SiOx superlattices in planar microcavities," J. Vac. Sci. Technol. B **16**, 1707 (1998).

[22]   D. J. Lockwood, B. T. Sullivan, and H. J. Labbe, "Visible light emission from Si/SiOx superlattices in optical microcavities," J. Lumin **80**, 75 (1999).

[23]   K. M. Cheng, A. W. Sparks, H.-C. Luan, D. R. Lim, K. Wada, and L. C. Kimerling, "SiO2/TiO2 omnidirectional reflector and resonator with sol-gel method," Appl. Phys. Lett. **75**, 3805 (1999).

[24]   F. Hamelmann, G. Haindl, J. Schmalhorst, A. Aschentrup, E. Majkova, U. Kleineberg, U. Heinzmann, A. Klipp, P. Jutzi, A. Anopchenko, M. Jergel, and S. Luby, "Metal oxide / silicon oxide multilayer with smooth interfaces produced by in situ controlled plasma enhanced MOCVD," Thin Solid Films **358**, 90 (2000).

[25]   L. Pavesi, R. Guardini, and C. Mazolleni, "Porous Silicon Resonant Cavity Light Emitting Diodes," Solid State Commun. **97**, 1051 (1996).

[26]   M. Araki, H. Koyama, and N. Koshida, "Controlled electroluminescence spectra of porous silicon diodes with vertical optical cavity," Appl. Phys. Lett. **69**, 2956 (1996).

[27]   D. Hunkel, R. Butz, R. Ares-Fisher, M. Marso, and H. Lüth, "Interference filters from porous silicon with laterally varying wavelength of reflection," J. Lumin. **80**, 133 (1999).

[28]   H. F. Arrand, T. M. Benson, P. Sewell, and A. Loni, "Optical waveguides in porous silicon pre-patterned by localized nitrogen implantation," J. Lumin. **80**, 199 (1999).

[29]   S. W. Leonard, H. M. van Driel, K. Busch, S. John, A. Birner, A.-P. Li, F. Müller, U Gösele, and V. Lehmann, "Attenuation of optical transmission within the band gap of thin two-dimensional macroporous silicon photonic crystals," Appl. Phys. Lett. **75**, 3063 (1999).

[30]   M. C. Netti, M. D. B. Charlton, G. J. Parker, and J. J. Baumberg, "Visible photonic band gap engineering in silicon nitride waveguides," Appl. Phys. Lett. **76**, 991 (2000).

[31]   Tsing-Hua Her, Richard J. Finlay, Claudia Wu, and Eric Mazur, "Femtosecond laser-induced formation of spikes on silicon", Appl. Phys. A 70, 383-385 (2000).

[32]   Tsing-Hua Her, Richard J. Finlay, Claudia Wu, Shrenik Deliwala, Eric Mazur, "Microstructuring of silicon with femtosecond laser pulses", Appl. Phys. Lett. 73, 1673-1675 (1998).

[33]   R. Williams, "Modern GaAs Processing Methods", (Artech House, Boston, 1990) pp. 153.

2.   Amorphous Silicon

Amorphous silicon is already an established material in semiconductor technology [34]. The major application of amorphous silicon is photovoltaics, color detectors, and active matrix displays. The primary attribute of the technology is its large area capability, which is unavailable with other technologies. Another advantage of amorphous silicon is that, it can be deposited by plasma enhanced chemical vapor deposition (PECVD) on almost any substrate at temperatures below 500 K, which makes it compatible with the microelectronic technology. This property justifies the interest in amorphous silicon as a potential optoelectronic material. Planar waveguides are already being realized from amorphous silicon [35].   With modern process techniques, it will be possible to integrate lasers, photodetectors, and waveguides into silicon motherboards [36,37] for wavelength division multiplexing (WDM) applications [38].

2.1.   Amorphous silicon synthesis

Hydrogen is included in the plasma deposited film, because silane is used as the silicon source. Although we refer to our plasma deposited material as "amorphous silicon", it contain N, because silane is mixed with a carrier gas, N_2. Oxygen may be present from background gases or water, carbon may be present from background hydrocarbons. So the resulting "amorphous silicon" includes Si, H, N, 0, and C. The recipe used to deposit approximately 1640 Å thick amorphous silicon layer is given in the below table. Ellipsometer can not measure the thickness and the refractive index of amorphous silicon. The thickness was measured by a surface texture analysis system to be 1640 ± 30 Å and the refractive index was estimated from the literature to be 2.18. [39, 40]

Parameter	Value
Automatic Pressure Controller (APC) Pressure	1000 m Torr
RF Power	20 W
Temperature	100°C
2% SiH_4 + 98% N_2 Flow Rate	180 sccm
Process Time	6.34 minutes

Table 2.1. Amorphous silicon PECVD recipe
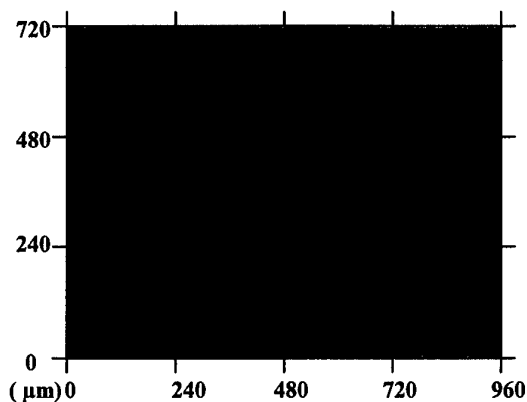
2.2. Surface morphology of the amorphous silicon

Figure 2.1 Optical microscope picture of amorphous silicon.

Atomic force microscopy (AFM) and optical microscopy (OM) have been performed the on the amorphous silicon samples to characterize the morphology of the surface and to analyze origin of the luminescence. The surface of the amorphous silicon is optically flat and thus amenable for the growth of multiple layers. The following figure shows a medium resolution AFM of the amorphous silicon surface.
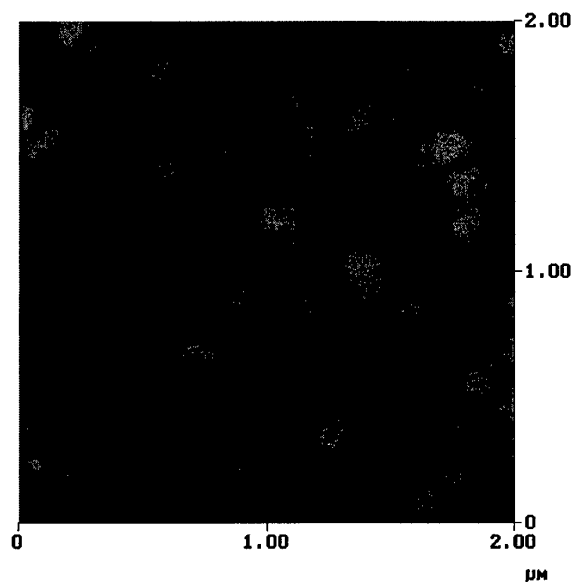

Figure 2.2. Medium resolution AFM of the amorphous silicon.

The surface morphology of the a-SiNx:H is quite uniform. The bulk of the material is composed of globules of a-SiNx:H and is similar porous silicon, which has similar luminescence properties.

2.3. Luminescence of amorphous silicon

The advantage of amorphous silicon is that, it attracts interest as a potential optical gain medium, because of its room temperature visible electroluminescence (EL) and photoluminescence (PL). Recently, we have observed visible PL from amorphous silicon, as well as its oxides and nitrides grown by low temperature PECVD. [41] While the exact mechanism of the occurrence of the PL in bulk amorphous silicon is still under discussion, the quantum confinement model is a widely accepted. [42] In the quantum confinement model the material consist of small silicon clusters in a matrix of amorphous silicon. The regions with Si-H and Si-N, having larger energy gaps due to strong Si-H and Si-N bonds, isolate these silicon clusters, and form barrier regions around them. The PL originates from the silicon clusters.

Amorphous silicon can be grown both with and without ammonia (NH_3). The samples grown without NH_3 are referred to as the Si rich samples. The luminescence of these samples is in the red-near-infrared part of the optical spectrum. The samples grown with NH_3 and annealed at 800° C are referred to as the nitrogen rich samples. The luminescence of these samples is in the blue-green part of the optical spectrum [43]. The following figure shows the room temperature PL amorphous silicon grown without NH_3. The PL spectrum has a linewidth of 250 nm and the peak of the PL is at 710 nm.
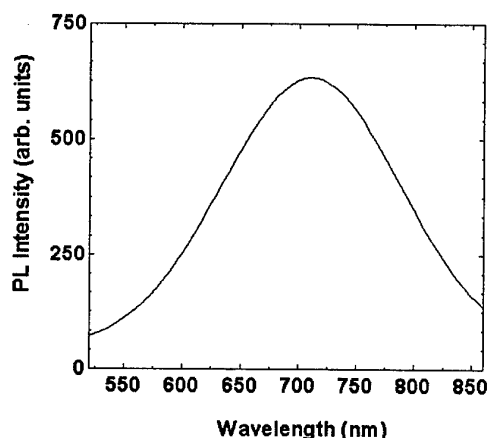

Figure 2.3. Room temperature PL of amorphous silicon.

2.4. Temperature dependence of the PL

The following figure shows the PL spectra of the amorphous silicon measured in the 550 - 900 nm wavelength and in the 12 – 298 K temperature range at a constant excitation laser intensity of 0.1 W cm^{-2}. A broad PL band centered at 710 nm (E_p = 1.746 eV) at 12 K is observed. The PL spectra have approximately a Gaussian lineshape modulated slightly by Fabry-Perot resonances. These resonances are due to the Fresnel reflections from the amorphous silicon film surfaces. The PL intensity decreases with increasing temperature. This feature is typical of the PL, which is due to donor-acceptor pair transitions observed in semiconductors [44].
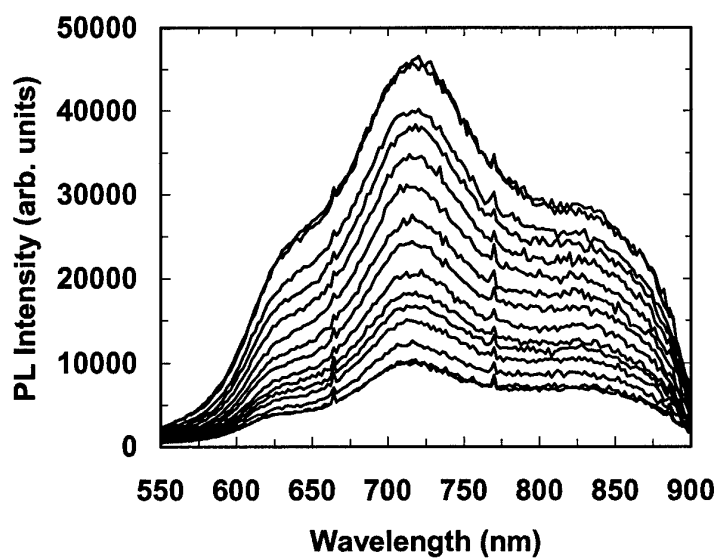
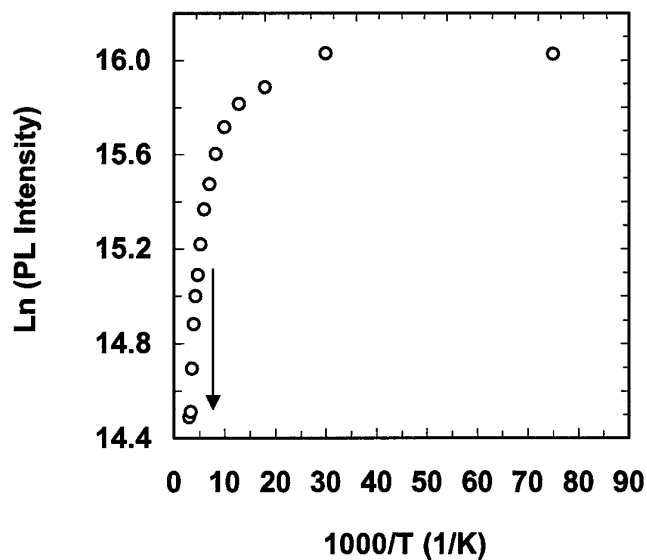Figure 2.4. PL spectra of a-SiNx:H in the 12 - 298 K temperature range.

Figure 2.5. Temperature dependence of amorphous silicon PL intensity at the emission band maximum. The arrow at 170 K shows the starting point of the intensive quenching.

The variation of the PL peak with respect to temperature is plotted in the previous figure. In the 12 - 170 K range, the PL intensity decreases slowly. Above 170 K, however, the PL intensity decreases at a larger rate due to a thermal quenching process. The activation energy ΔE for this thermal quenching process can be derived in the 170 - 298 K temperature range using a nonlinear least squares fit to the following equation, $I = I_0 \exp(\Delta E / k_B T)$, where I is the PL intensity, I_0 a proportionality constant, and k_B the Boltzmann's constant. The semilog plot of the emission band intensity as a function of the reciprocal temperature gives a straight line in the 170 - 298 K region. An activation energy of $E_a = 0.027$ eV for the emission band is derived from the slope of the straight line fit. This activation energy is associated with a shallow level located at 0.027 eV from the band. This shallow level in undoped amorphous silicon may be associated with the presence of defects and unintentional impurities [45].

2.5. Power dependence of the PL

The following figure presents the PL spectra for 10 different laser intensities at 12 K. As the power is increased the PL intensity increases.
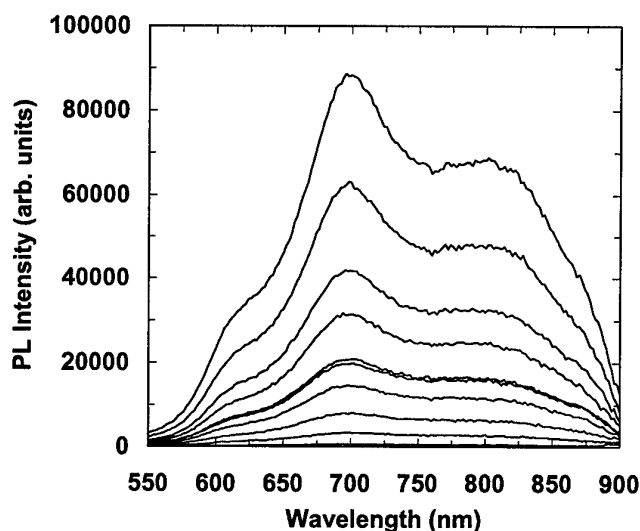

Figure 2.6. PL spectra of a-SiN$_x$:H in the $0.1 - 3.7$ W cm^{-2} laser intensity range at 12 K.

The intensity variation of the emission band versus the excitation laser intensity at T = 12 K is also investigated and plotted in the following figure. The experimental data can be fitted by a simple power law, $I \propto L^\gamma$, where I is the PL intensity, L the excitation laser intensity, and γ a dimensionless exponent. It was found that, the PL intensity increases sublinearly (i.e., $\gamma = 0.89$) with respect to the excitation laser intensity. For an excitation laser photon with an energy exceeding the band gap energy E_g, the coefficient γ is generally $1 < \gamma < 2$ for the free- and bound-exciton emission, and $\gamma \leq 1$ for free-to-bound and donor-acceptor pair recombination [46]. Thus, the obtained value of $\gamma = 0.89$ confirms the assignment of the observed emission band in amorphous silicon is due to donor-acceptor pair recombination.
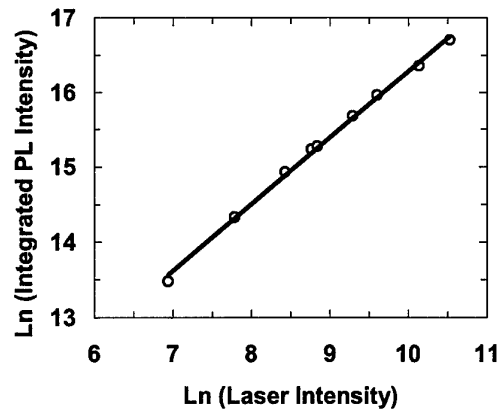
Figure 2.7. Dependence of amorphous silicon integrated PL intensity versus excitation laser intensity at 12 K. The solid curve gives the theoretical fit using Eq. $I \propto L^{\gamma}$.

2.6. References

[34] R. A. Street, Ed., "Technology and Applications of Amorphous Silicon," (Springer Verlag, Berlin, 2000), pp. 1-403.

[35] A. M. Agarwal, L. Liao, J. S. Foresi, M. R. Black, X. Duan, and L.C. Kimerling, "Low-loss Polycrystalline Silicon Waveguides for Silicon Photonics," J. Appl. Phys. **80**, 6120 (1996).

[36] B. Jalali, S. Yegnanarayanan, T. Yoon, T. Yoshimoto, I. Rendina, and F. Coppinger, "Advances in Silicon on insulator Optoelectronics," IEEE J. Select. Topics in Quantum Electron. **4**, 938 (1998).

[37] A. Kaneko, T. Goh, H. Yamada, T. Tanaka, and I. Ogawa "Design and applications of silica-based planar lightwave circuits," IEEE J. Select. Topics in Quantum Electron. **5**, 1227 (1999).

[38] B. J. Offrein, R. Germann, F. Horst, H.W.M. Salemink, R. Beyerl, and G. L. Bona, "Resonant coupler-based tunable add-after-drop filter in silicon–oxynitride technology for WDM networks," IEEE J. Select. Topics in Quantum Electron. **5**, 1400 (1999).

[39] A. Serpengüzel, A. Aydinli, and Alpan Bek, "Enhancement and Inhibition of Photoluminescence in Hydrogenated Amorphous Silicon Nitride Microcavities", Opt. Express **1**, 108 (1997).

[40]   A. Serpengüzel, A. Aydinli, and Alpan Bek, "Alteration of Spontaneous Emission in hydrogenated Amorphous Silicon Microcavities", J. Non-Crystalline Solids, **227-230**, 1142-1145 (1998).

[41]   A. Serpengüzel, A. Aydinli, and A. Bek, "Enhancement and inhibition of photoluminescence in hydrogenated amorphous silicon nitride microcavities, " Optics Express **1**, 108 (1997).

[42]   M. H. Brodsky, "Quantum Well Model of the Hydrogenated Amorphous Silicon," Solid State Commun. **36**, 55 - 59 (1980).

[43]   A. Serpengüzel, A. Aydinli, A. Bek, and M. Güre, "Visible photoluminescence from planar amorphous silicon nitride microcavities, " J. Opt. Soc. Am. B. **15**, 2706 (1998).

[44]   H.G. Kim, K.H. Park, B.N. Park, H.J. Lim, S.K. Min, H.L. Park, W.T. Kim, Jap. J. Appl. Phys. **32**, 476 (1993).

[45]   V. Capozzi, Phys. Rev. B **28** 4620 (1983).

[46]   T. Schmidt, K. Lischka, W. Zulehner, Phys. Rev. B **45** 8989 (1992).

3. Porous Silicon

Porous silicon has been the subject of detailed and wide-ranging studies over the last 13 years due to its unusual and interesting optoelectronic properties, but the origins of this material go back more than 35 years. It has only recently been recognized that the optical properties of porous silicon are significantly different from those of crystalline bulk silicon. Porous silicon exhibits efficient room temperature photoluminescence in the red region (1.4 - 2.2 eV) of the visible spectrum.

Crystalline silicon is an indirect bandgap semiconductor and has little efficiency in light emission. However, the optical properties of porous silicon are significantly different from those of bulk crystalline silicon. In 1990 Canham found efficient and strong room temperature photoluminescence (PL) in porous silicon [47]. Canham realized that in fresh porous silicon the quantum confinement effects play a major role in the appearance of this efficient luminescence as the width of the wire-like microstructures were small enough, that is, on the order of < 5nm. The PL can usually be seen with the naked eye. This effect has attracted a great number of research activities over the last decade. Technologically, these activities occurred because of the vision of an all-silicon-based optoelectronics.

3.1. Porous silicon synthesis

The common technique to form a porous silicon layer from a bulk crystalline silicon is to use an electrochemical process. Porous silicon can be fabricated from n-type and p-type crystalline silicon by using electrochemical anodization of monocrystalline silicon in hydrofluoric (HF) acid based solutions [48]. Porous silicon is generally made up of a (100) p-type silicon wafer, whose resistivity is between 1-10 Ω cm. First of all, etching is performed in an electrolyte consisting of HF/HNO_3/water = 1:3:5. This step is done to leave smooth surfaces. In the second step, anodization, pores are created. The silicon wafer is subjected to a dc current while immersed in a HF based solution of HF/ethanol/water = 1:2:1 by volume at normal temperatures. The main aim to use ethanol in the anodization process is to remove hydrogen gas from the porous silicon surface. Current densities are in the range of 20 mA/cm^2. The remaining porous layer is a complicated network of silicon wires each with a thickness of between 2-5 nm. This process is summarized in the following table [49].

Parameter	Value
Take HF of high concentration as an electrolyte	> 10 %
Use homogenously doped p-type Si substrates	$10^{15} - 10^{17}$ cm^{-3}
Keep the formation current density constant	$10 - 100\ ^{mA}\!/\!_{cm^2}$
Anodize in the dark	0 lux

Table 3.2. Porous silicon electrochemical etch recipe.
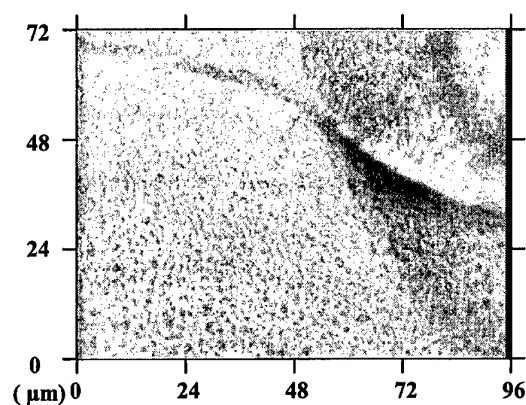
3.2. Surface morphology of porous silicon

Figure 3.1 Optical microscope picture of porous silicon.

Atomic force microscopy (AFM) and optical microscopy (OM) have been performed the on the porous silicon samples to characterize the morphology of the surface and to analyze origin of the luminescence. The surface of the porous silicon is rather rough. The bulk of the material is composed of globules of as we have seen in porous silicon. The following figure shows the medium resolution AFM picture of the porous silicon surface.
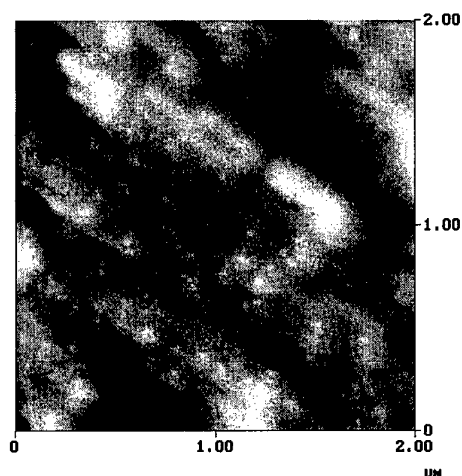
Figure 3.2 Medium resolution AFM of the porous silicon surface.

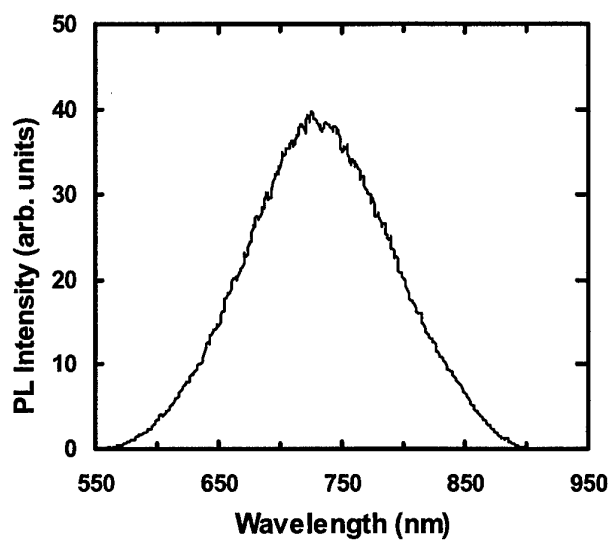## 3.3. Luminescence of porous silicon

Figure 3.3. PL spectrum of porous silicon at room temperature.

The previous figure shows the PL spectra of the porous silicon measured in the 550 - 900 nm wavelength at 300 K at an excitation laser intensity of 0.005 W cm^{-2}. A broad PL band centered at 725 nm (E_p = 1.710 eV) at 300 K is observed. The PL spectrum has approximately a Gaussian lineshape.
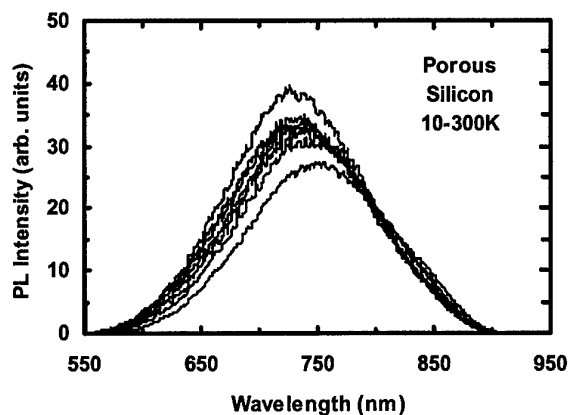
3.4.   Temperature dependence of the PL

Figure 3.4. PL spectra of porous silicon in the 10 - 300 K temperature range.

The previous figure shows the PL spectra of the porous silicon measured in the 550 - 900 nm wavelength and in the 10 - 300 K temperature range at a constant excitation laser intensity of 0.005 W cm^{-2}. A broad PL band centered at 750 nm (E_p = 1.698 eV) at 10 K is observed. The PL spectra have approximately a Gaussian lineshape.
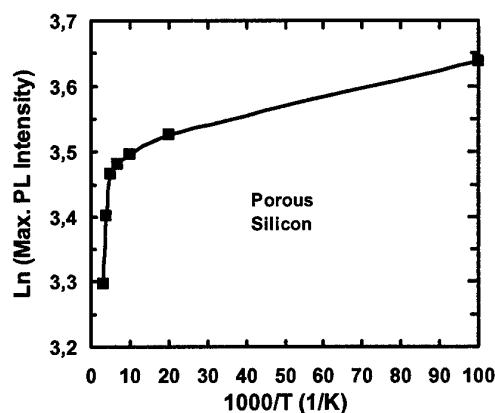

Figure 3.5. Temperature dependence of porous silicon PL intensity at the emission band maximum. Intensive quenching starts at 200 K.

The PL intensity decreases with increasing temperature. This feature is typical of the PL, which is due to donor-acceptor pair transitions observed in semiconductors. The variation of the PL peak with respect to temperature is plotted in the previous figure. In the 10 - 150 K range, the PL intensity decreases slowly. Above 200 K, however, the PL intensity decreases at a larger rate due

to a thermal quenching process. The activation energy ΔE for this thermal quenching process can be derived in the 200 - 300 K temperature range using a nonlinear least squares fit to the following equation, $I = I_0 \exp(\Delta E/k_B T)$, where I is the PL intensity, I_0 a proportionality constant, and k_B the Boltzmann's constant. The semilog plot of the emission band intensity as a function of the reciprocal temperature gives a straight line in the 200 - 300 K region. An activation energy of $E_a = 0.009$ eV for the emission band is derived from the slope of the straight line fit. This activation energy is associated with a shallow level located at 0.009 eV from the band. This shallow level in porous silicon may be associated with the presence of defects and unintentional impurities.

3.5.   Power dependence of the PL

The following figure presents the PL spectra for different laser intensities at 10 K. As the power is increased the PL intensity increases.
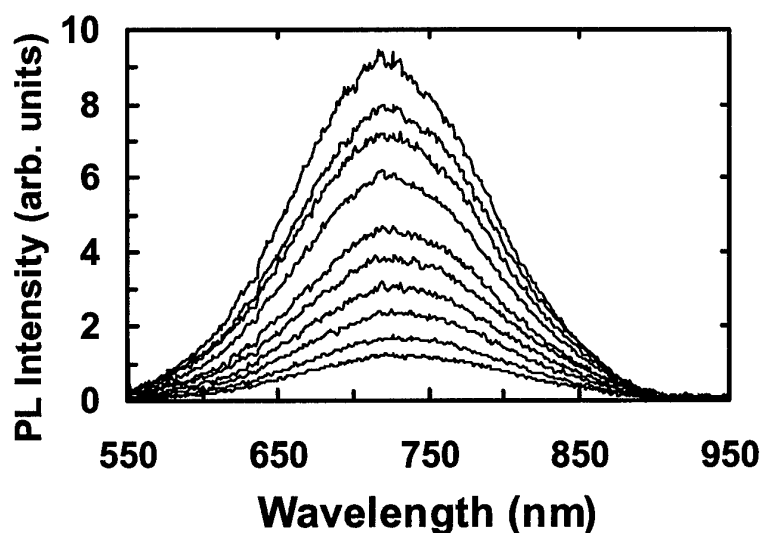

Figure 3.6. PL spectra of the porous silicon 1.4 – 5.75 W cm^{-2} laser intensity range at 10 K.

The intensity variation of the emission band versus the excitation laser intensity at T = 10 K is also investigated and plotted in the following figure. The experimental data can be fitted by a simple power law, $I \propto L^{\gamma}$, where I is the PL intensity, L the excitation laser intensity, and γ a dimensionless exponent. It was found that, the PL intensity increases superlinearly (i.e., $\gamma = 1.44$) with respect to the excitation laser intensity. For an excitation laser photon with an energy exceeding the band gap energy E_g, the coefficient γ is generally $1 < \gamma < 2$ for the free- and bound-exciton emission, and $\gamma \leq 1$ for free-to-bound and donor-acceptor pair recombination [50]. Thus, the obtained value of $\gamma = 1.44$ confirms the assignment of the observed emission band in porous silicon is due to free-to-bound and donor-acceptor pair recombination.
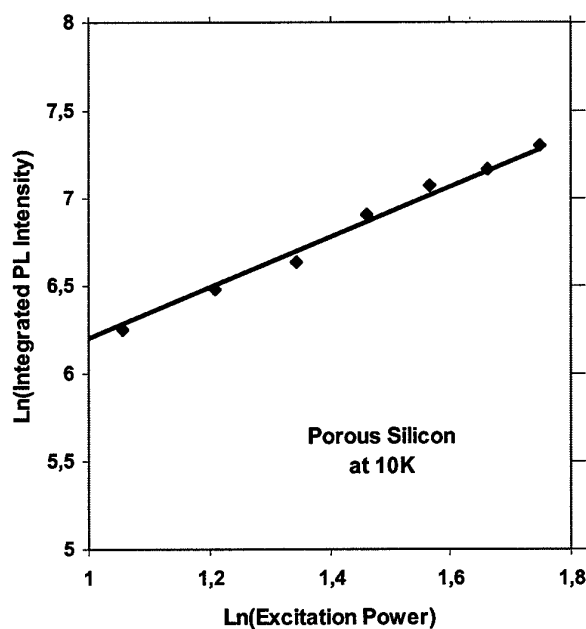
Figure 3.7. Dependence of porous silicon integrated PL intensity versus excitation laser intensity at 10 K. The solid curve gives the theoretical fit using Eq. $I \propto L^{\gamma}$.

3.6. References

[47] L.T. Canham, "Silicon Quantum Wire Array Fabrication by Electrochemical and Chemical Dissolution of Wafers," Appl. Phys. Lett. 57, 1046-1048 (1990).

[48] M. Ohmukai, Y. Nishiguchi, and Y. Tsutsumi, "The Dependence of Hydrofluoric Acid Concentration during Anodization on Photoluminescence of Porous Silicon," Sci. and Tech. of Adv. Mat. 2, 455-457 (2001).

[49] Z.C. Feng, R. Tsu, "Porous Silicon," World Scientific Publishing, Singapore, 27 (1994).

[50] T. Schmidt, K. Lischka, W. Zulehner, Phys. Rev. B 45 8989 (1992).

4. Black Silicon

Silicon is the material of computer chips and solar cells. It is ubiquitous throughout the high-tech world. Ordinarily, silicon absorbs a moderate amount of visible light, but a substantial amount of visible light is reflected as well, and infrared and ultraviolet light are transmitted through silicon or reflected from it with very little absorption.
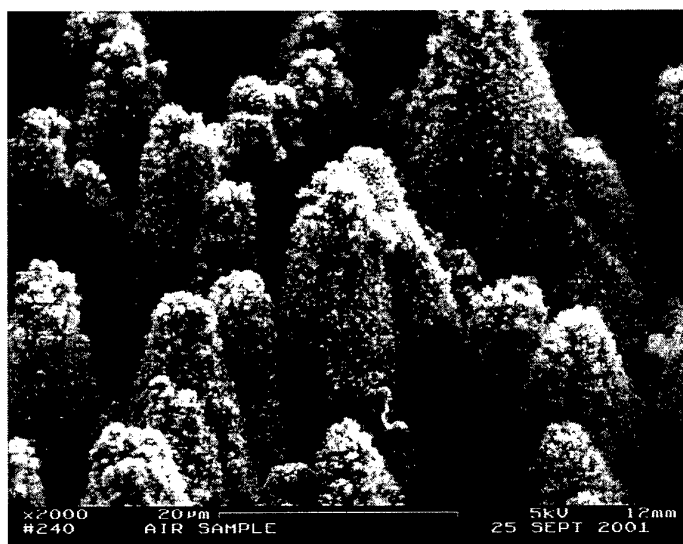

Figure 4.1. Scanning electron microgram of black silicon.

Spiked silicon surfaces, in contrast, absorb nearly all light at wavelengths ranging from the ultraviolet to the infrared. This suggests it may be very useful in improving the performance of existing silicon devices, such as detectors and photovoltaics. Spiked silicon is made by shining a series of very short, very intense laser pulses at a silicon surface in a chamber filled with a gas such as sulfur hexafluoride or chlorine. In the presence of the laser light, the gas reacts with the silicon surface etches away some of it, leaving a pattern of conical spikes behind.

4.1. Black silicon synthesis

Mazur's group recently [51,52] discovered that irradiation of silicon surfaces with femtosecond laser pulses in the presence of a halogen containing gas transforms the flat, mirror-like surface of a silicon wafer into a forest of microscopic spikes. The spiked surface is strongly light-absorbing: the surface of silicon, normally gray and shiny, turns deep black. The spikes are tens of micrometers tall and have tip sizes on the order of hundreds of nanometers.

Spike formation depends strongly on the characteristics of the laser pulses: they must be ultrashort and very intense. Also, the halogen gas in which the silicon is placed during the irradiation is critical. The importance of the surrounding gas suggests that chemical reactions are involved in the formation of the spikes. The crystal structure of the substrate does not appear to be important, since spikes form on both Si(100) and Si(111); the interaction of the laser with the surface seems to determine which parts of the surface react most with the gas.

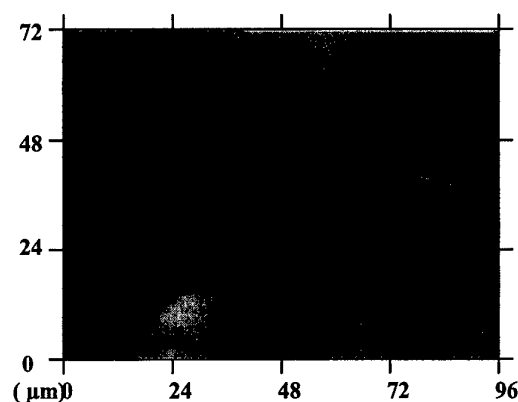## 4.2.   Surface morphology of black silicon

Figure 4.2. Optical microscope picture of black silicon.

Atomic force microscopy (AFM) and optical microscopy (OM) have been performed the on the black silicon samples to characterize the morphology of the surface and to analyze origin of the luminescence. The surface of the black silicon is optically black and consists of conical layers. The bulk of the material is composed of globules of black silicon and is similar to porous silicon. The following figure shows the medium resolution AFM picture of the black silicon surface.
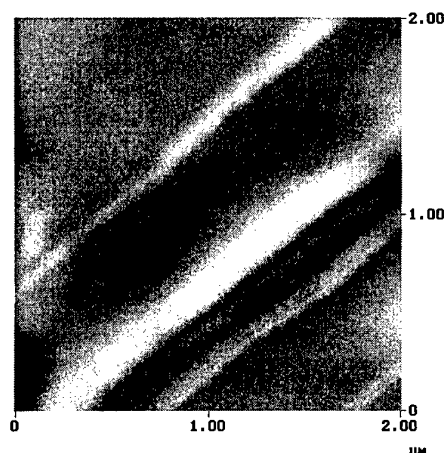

Figure 4.3. Medium resolution AFM of the black silicon surface.

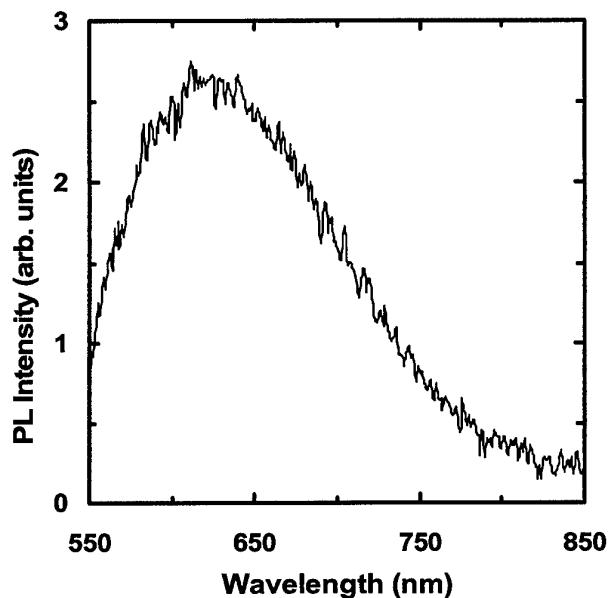## 4.3. Luminescence of black silicon

Figure 4.4. PL spectra of black silicon at 300 K.

The previous figure shows the PL spectrum of the black silicon measured in the 550 - 850 nm wavelength and at room temperature at a excitation laser intensity of 0.1 W cm^{-2}. A broad PL band centered at 625 nm (E_p = 1.984 eV) at 300 K is observed. The PL spectrum has a left skewed Gaussian lineshape.

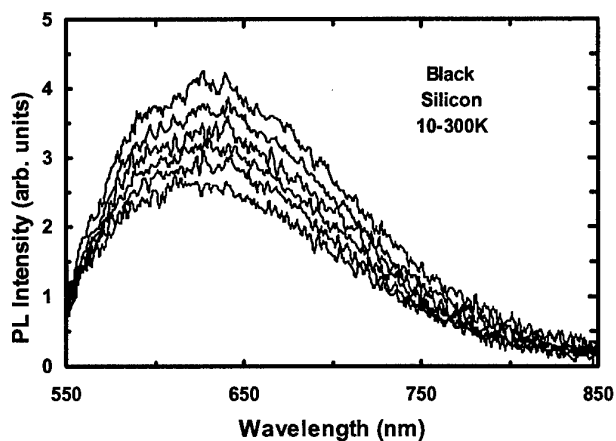## 4.4. Temperature dependence of the PL

Figure 4.5. PL spectra of black silicon in the 10 - 300 K temperature range.

The previous figure shows the PL spectra of the black silicon measured in the 550 - 850 nm wavelength and in the 10 – 300 K temperature range at a constant excitation laser intensity of 0.1 W cm^{-2}. A broad PL band centered at 630 nm (E_p = 1.968 eV) at 10 K is observed. The PL spectra have approximately Gaussian lineshape. The PL intensity decreases with increasing temperature. The variation of the PL peak with respect to temperature is plotted in the following figure. In the 10 - 120 K range, the PL intensity decreases slowly. Above 120 K, however, the PL intensity decreases at a larger rate due to a thermal quenching process. The activation energy ΔE for this thermal quenching process can be derived in the 120 - 300 K temperature range using a nonlinear least squares fit to the following equation, I = I$_o$ exp (ΔE/k$_B$T), where I is the PL intensity, I$_o$ a proportionality constant, and k$_B$ the Boltzmann's constant. The semilog plot of the emission band intensity as a function of the reciprocal temperature gives a straight line in the 120 - 300 K region. An activation energy of E$_a$ = 0.006 eV for the emission band is derived from the slope of the straight line fit. This activation energy is associated with a shallow level located at 0.006 eV from the band. This shallow level in black silicon may be associated with the presence of defects and unintentional impurities.
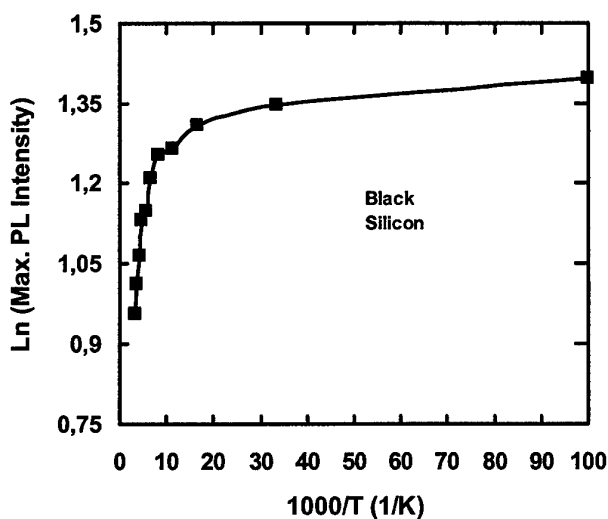

Figure 4.6. Temperature dependence of black silicon PL intensity at the emission band maximum.
Intensive quenching starts at 120 K.

4.5. Power dependence of the PL

The following figure presents the PL spectra for different laser intensities at 10 K. As the power is increased the PL intensity increases.
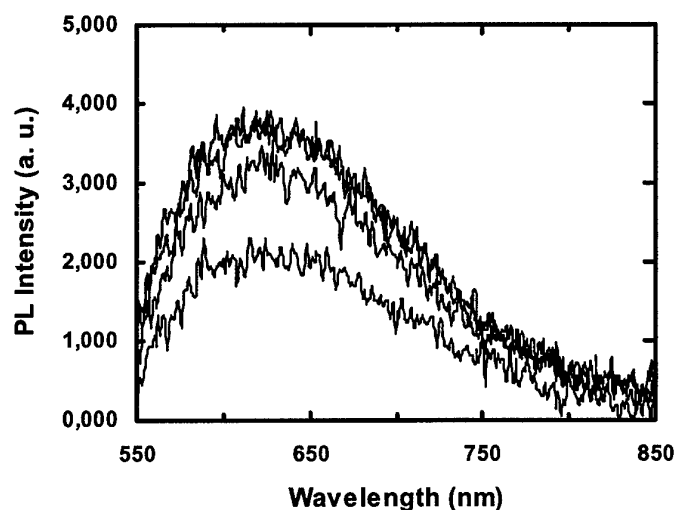
Figure 4.7. PL spectra of black silicon 5.75-23.0 MW cm^{-2} laser intensity range at 10 K.

The intensity variation of the emission band versus the excitation laser intensity at T = 10 K is also investigated and plotted in the following figure. The experimental data can be fitted by a simple power law, I $\propto$ L$^\gamma$, where I is the PL intensity, L the excitation laser intensity, and γ a dimensionless exponent. It was found that, the PL intensity increases sublinearly (i.e., γ = 0.44) with respect to the excitation laser intensity. For an excitation laser photon with an energy exceeding the band gap energy E$_g$, the coefficient γ is generally 1 < γ < 2 for the free- and bound-exciton emission, and γ ≤ 1 for free-to-bound and donor-acceptor pair recombination [53]. Thus, the obtained value of γ = 0.44 confirms the assignment of the observed emission band in a-SiN$_x$:H is due to donor-acceptor pair recombination.
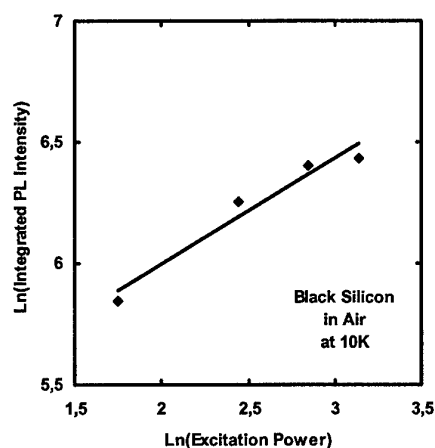

Figure 4.8. Dependence of black silicon integrated PL intensity versus excitation laser intensity at 10 K. The solid curve gives the theoretical fit using Eq. $I \propto L^\gamma$.

4.6. References

[51]   Tsing-Hua Her, Richard J. Finlay, Claudia Wu, and Eric Mazur, "Femtosecond laser-induced formation of spikes on silicon", Appl. Phys. A 70, 383-385 (2000).

[52]   Tsing-Hua Her, Richard J. Finlay, Claudia Wu, Shrenik Deliwala, Eric Mazur, "Microstructuring of silicon with femtosecond laser pulses", Appl. Phys. Lett. 73, 1673-1675 (1998).

[53]   T. Schmidt, K. Lischka, W. Zulehner, Phys. Rev. B **45** 8989 (1992).

5. Conclusions

Amorphous silicon is grown by plasma enhanced chemical vapor deposition (PECVD) on silicon substrates. Porous silicon is obtained from crystalline silicon by electrochemical etching. Black silicon is obtained from crystalline silicon by femtosecond laser processing. The temperature and power dependence of the amorphous, porous, and black silicon photoluminescence is performed to fully characterize and optimize the material in the pursuit of obtaining novel photonic microdevices. Atomic force microscopy (AFM) is used for morphological material characterization. Such fundamental studies are important for the development of novel optoelectronic devices with increased efficiency, speed, and bandwidth.

Photonic devices manufactured using amorphous, porous, and black silicon have potential optoelectronic applications such as flat panel or heads-up displays, wavelength division multiplexing (WDM) light sources and detectors, nanocavity lasers, optical add-drop filters, optical couplers and waveguides, and diffractive optical elements. The following figure shows the color mixing diagram. Devices producing the three main colors (RGB) can be used to produce the whole optical spectrum.
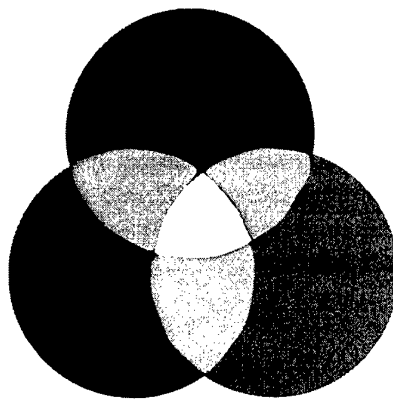
Figure 5.1. Color mixing diagram.

Currently, these devices exist as discrete photonic elements. However, in the near future, they will be integrated into nanofabricated photonic integrated circuits (PIC's) operating at visible and near-infrared (near-IR) wavelengths. These integrated devices are essential for the high speed and high capacity information superhighway. With the incorporation of integrated services digital network (ISDN) architecture into our daily environment, we will need this optical communication infrastructure in the next decade. Additional device applications may include physical, chemical, and biological agent detection.
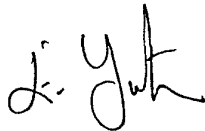
In this project, bulk luminescence properties of amorphous, porous, and black silicon were studied at room temperature and at low temperatures. The PL emission intensity increases at low temperatures due to the lack of thermally excited phonons. The emission spectrum stays broad even at low temperatures. The broad luminescence spectrum even at low temperatures is a results of the heterogenous size distribution of the amorphous silicon quantum dots. This heterogenous size distribution is further confirmed by atomic force microscopy (AFM) and optical microscopy (OM) measurements of the sample surfaces. The photoluminescence (PL) extends from the red part of the spectrum to the near-infrared for the samples. The broad PL spectrum of the amorphous, porous, and black silicon, makes them suitable sources for wavelength division multiplexing (WDM) applications as well as display applications.

Federal Acquisition Regulation Clauses

(1) In accordance with Defense Federal Acquisition Regulation 252.227-7036, Declaration of Technical Data Conformity (Jan 1997), All technical data delivered under this contract shall be accompanied by the following written declaration:

"The Contractor, Koc University, hereby declares that, to the best of its knowledge and belief, the technical data delivered herewith under Contract No. FA8655-02-M-4086 is complete, accurate, and complies with all requirements of the contract."
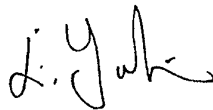
DATE: March 30, 2004

Name and Title of Authorized Official: Dr. Ersin Yurtsever, Professor and Dean

(End of Clause)

(2) In accordance with the requirements in Federal Acquisition Regulation 52.227-13, Patent Rights-Acquisition by the U.S. Government (Jun 1989), CONTRACTOR WILL INCLUDE IN THE FINAL REPORT ONE OF THE FOLLOWING STATEMENTS:

(A) "Disclosures of all subject inventions as defined in FAR 52.227-13 have been reported in accordance with this clause."

DATE: March 30, 2004

Name and Title of Authorized Official: Dr. Ersin Yurtsever, Professor and Dean

(End of Clause)